

---

# Robust Quantity-Aware Aggregation for Federated Learning

---

Jingwei Yi<sup>1</sup> Fangzhao Wu<sup>2</sup> Huishuai Zhang<sup>2</sup> Bin Zhu<sup>2</sup> Tao Qi<sup>3</sup>  
Guangzhong Sun<sup>1</sup> Xing Xie<sup>2</sup>

<sup>1</sup>University of Science and Technology of China, Hefei 230026, China

<sup>2</sup>Microsoft Research Asia, Beijing 100080, China

<sup>3</sup>Department of Electronic Engineering, Tsinghua University, Beijing 100084, China

yjw1029@mail.ustc.edu.cn taoqi.qt@gmail.com gzsun@ustc.edu.cn

{fangzhu, huzhang, binzhu, xingx}@microsoft.com

## Abstract

Federated learning (FL) enables multiple clients to collaboratively train models without sharing their local data, and becomes an important privacy-preserving machine learning framework. However, classical FL faces serious security and robustness problem, e.g., malicious clients can poison model updates and at the same time claim large quantities to amplify the impact of their model updates in the model aggregation. Existing defense methods for FL, while all handling malicious model updates, either treat all quantities benign or simply ignore/truncate the quantities of all clients. The former is vulnerable to quantity-enhanced attack, while the latter leads to sub-optimal performance since the local data on different clients is usually in significantly different sizes. In this paper, we propose a robust quantity-aware aggregation algorithm for federated learning, called FedRA, to perform the aggregation with awareness of local data quantities while being able to defend against quantity-enhanced attacks. More specifically, we propose a method to filter malicious clients by jointly considering the uploaded model updates and data quantities from different clients, and performing quantity-aware weighted averaging on model updates from remaining clients. Moreover, as the number of malicious clients participating in the federated learning may dynamically change in different rounds, we also propose a malicious client number estimator to predict how many suspicious clients should be filtered in each round. Experiments on four public datasets demonstrate the effectiveness of our FedRA method in defending FL against quantity-enhanced attacks. Our code is available at <https://anonymous.4open.science/r/FedRA-4C1E>.

## 1 Introduction

Federated learning (FL) is an effective technology to train models while protecting the privacy of training data. It has been widely studied for many application scenarios, e.g., medical health [22, 23], keyboard prediction [29, 8] and personalized recommendation [19, 20, 30]. One of the classic FL algorithms is FedAvg [15]. In FedAvg, a central server iteratively samples a group of clients and distributes an aggregated global model to them. Clients train the model with their local datasets and upload their model updates to the server. Finally, the server averages the clients' updates with some weights determined by the *quantity* of each client, which means throughout the paper the number of the training data at that client, to update the global model.

The linear aggregation applied in FedAvg has been proved to be vulnerable to poisoning attacks [2, 7, 26, 28, 3]. The malicious clients not only can conduct various attacks on local training and submit

malicious updates to degrade the performance of the global model or inject a backdoor to the global model, but also can amplify the impact of malicious updates on the global model by submitting large quantities to obtain unfairly high weights in the model aggregation on the server. We name the attacks quantity-enhanced attacks throughout the paper.

Several methods have been proposed to defend against poisoning attacks for federated learning [4, 31, 6, 25, 17, 18]. However, most existing defenses are flawed in handling quantities. These methods can be classified into two groups according to their handling of quantities. The first group is quantity-ignorant defenses. Such a defense aggregates updates without considering quantities. Since aggregating updates with quantities benefits model performance [32, 21], applying these defenses may lead to performance degradation. For example, Yin et al. [31] propose Median and Trmean, which compute the median and trimmed-mean value of each dimension of the updates, respectively. Blanchard et al. [4] propose Krum, which selects the update closest to its subset of neighboring updates as the aggregated result. The second group is quantity-aware defenses. A defense in this group aggregates updates with quantities but by default treats quantities submitted by clients as benign. These defenses usually outperform quantity-ignorant defenses when quantities are submitted correctly. However, an attacker can exploit this characteristic to conduct quantity-enhanced attacks, leading to severely degraded performance of these quantity-aware defenses. For example, Sun et al. [25] propose Norm-Bound, which clips the norm of each update and averages them according to weights proportional to the quantities submitted by clients. Pillutla et al. [17] propose RFA, which runs an approximate algorithm to minimize the quantity-aware geometric median of updates.

In this paper, we propose a robust quantity-aware aggregation method, called *FedRA*, for federated learning. It aims to apply weighted averaging on updates according to clients' quantities, while being quantity-robust to defend FL against quantity-enhanced attacks. In FedRA, we propose a method to filter malicious clients by jointly considering the uploaded model updates and data quantities from different clients, and performing quantity-aware weighted averaging on model updates from remaining clients. Meanwhile, we notice that some existing defenses assume that the number of malicious clients in each round is fixed, which is too idealistic for federated learning. Therefore, we further propose a malicious client number estimator to dynamically decide the number of malicious clients in each round. Experiments on four datasets validate the effectiveness of our FedRA.

## 2 Related Works

Federated learning [15] enables multiple clients collaboratively train models without sharing their local datasets. There are three steps in each round of federated learning. First, a central server randomly samples a group of clients and distributes the global model to them. Second, the clients train the model with their local datasets and upload their model updates to the central server. Finally, the central server aggregates the received updates to update the global model. In FedAvg [15], the updates are weighted averaged according to the quantity of clients' training samples. The above steps are performed iteratively until the global model converges.

However, the classical federated learning is vulnerable to poisoning attacks, i.e., untargeted attacks [2, 7] and backdoor attacks [14, 1, 26, 28, 3]. In this paper, we focus on defending against untargeted attacks, which aim to degrade the performance of the global model on all input samples. To defend against the attacks, several robust aggregation methods have been proposed. Yin et al. [31] propose Median and Trmean that apply coordinated-wise median and trimmed-mean, respectively, to filter malicious updates. Blanchard et al. [4] propose Krum that computes a square-distance-based score to select the update closest to a subset of neighboring updates. mKrum [4] is a variance of Krum. It selects multiple updates and averages them. Bulyan [6] is a combination of mKrum and Trmean: it first selects several updates through mKrum and then aggregates them with Trmean. Since the above defenses do not consider quantities of clients' training samples, the convergence speed and model performance of these methods are degraded [32, 21], especially in long-tailed data distributions (see Appendix C.1). Long-tailed data distributions are common in real-world scenarios and have been widely researched [33, 34, 12]. These five methods are quantity-ignorant methods.

Sun et al. [25] propose Norm-bound that clips the  $L_2$  norm of received updates to a predefined threshold. Pillutla et al. [17] propose RFA that computes weights for each update by running an approximation algorithm to minimize the quantity-aware geometric median of updates. These two methods are quantity-aware defenses. They take quantities into consideration when aggregating

Table 1: Comparison of different defense methods in handling local data quantity.

	Krum	mKrum	Median	Trmean	Bulyan	Norm-bound	RFA	Truncate	ours
Quantity-aware	✗	✗	✗	✗	✗	✓	✓	✓	✓
Quantity-robust	✗	✗	✗	✗	✗	✗	✗	✓	✓
Joint detection	✗	✗	✗	✗	✗	✗	✗	✗	✓

updates but by default treat all received quantities as benign. Portnoy et al. [18] point out that received quantities may be malicious and can be exploited to increase the impact of malicious updates. They further propose to truncate received quantities to a dynamic threshold in each round, which guarantees any 10% clients do not have more than 50% samples. The Truncate method is quantity-robust. However, quantities of benign clients with a large number of training samples may also be truncated, which degrades performance. Meanwhile, they filter malicious updates without jointly considering quantities and updates. It cause the assumptions in Trmean may not hold, which leads to sub-optimal update filtering. We summarize the characteristics of defenses in Table 1.

### 3 Problem Definition

Suppose that training samples are sampled from a distribution  $\mathcal{D}$  in sample space  $\mathcal{Z}$ . Let  $f(\mathbf{w}; z)$  denote the loss function of model parameter  $\mathbf{w}$  at data point  $z$ , and  $F(\mathbf{w}) = \mathbb{E}_{z \sim \mathcal{D}}[f(\mathbf{w}; z)]$  is the corresponding population loss function. The goal is to train a model that minimizes the population loss function  $\mathbf{w}^* = \arg \min_{\mathbf{w} \in \mathcal{W}} F(\mathbf{w})$  in the parameter space. Assume that there are  $N$  clients in total and  $M$  of them are malicious. The  $i$ -th client has a local dataset  $D_i$ , where any  $z \in D_i$  are independently sampled from distribution  $\mathcal{D}$ . The empirical loss of the  $i$ -th client is  $F_i(\mathbf{w}) = \frac{1}{|D_i|} \sum_{z \in D_i} f(\mathbf{w}; z)$ . In the  $t$ -th round, the central server randomly samples  $n$  clients and distributes the global model  $\mathbf{w}_t$  to them. To simplify the theoretical analysis, we follow FedSGD [15] and Trmean [31], and assume that if the  $i$ -th client is benign, its update is  $\mathbf{g}_t^i = \nabla F_i(\mathbf{w}_t)$  and its quantity is  $q_t^i = |D_i|$ . If the  $i$ -th client is malicious, it can submit an arbitrary update and quantity to the server. After receiving the updates and quantities from the sampled  $n$  clients, the server computes the global update with a certain aggregation rule  $\mathcal{A}$ :  $\mathbf{g}_{t+1} = \mathcal{A}(\mathbf{g}_t^1, \dots, \mathbf{g}_t^n, q_t^1, \dots, q_t^n)$ .

Some of the existing defenses, e.g., mKrum [4] and Trmean [31], need to know the number of malicious clients in each round to set parameters appropriately. However, this is unrealistic in federated learning scenarios. In our work, we consider two settings: fixed-ratio setting and dynamic-ratio setting. In the fixed-ratio setting, the number of malicious clients  $m$  in each round is proportional, i.e.,  $m = \lceil \frac{nM}{N} \rceil$ . It is known to the server. This setting is unrealistic in federated learning. We use it to analyze the upper bound capability of defenses to filter malicious updates. In the dynamic-ratio setting, the server only knows the overall number of malicious clients  $M$ , but the exact number of malicious clients in each round is unknown. Compared to the fixed ratio setting, the dynamic ratio setting is more in line with real-world federating learning scenarios.

We introduce some definitions that are useful in describing our algorithm.

**Definition 1** ( $(r, m)$ -Byzantine resilience). Let  $\mathbf{g}^1, \dots, \mathbf{g}^{n-m}$  be independent identically distributed random vectors, where  $\mathbf{g}^i \in \mathbb{R}^d$ , and  $\mathbb{E}[\mathbf{g}^i] = \boldsymbol{\mu}$ . Let  $\mathbf{b}^1, \dots, \mathbf{b}^m$  be any random vectors in  $\mathbb{R}^d$ , possibly dependent on  $\mathbf{g}^i$ s. Aggregate rule  $\mathcal{A}$  is said to be  $(r, m)$ -Byzantine resilience if  $\mathbf{g} = \mathcal{A}(\mathbf{g}^1, \dots, \mathbf{g}^{n-m}, \mathbf{b}^1, \dots, \mathbf{b}^m)$  satisfies  $\mathbb{E}[\|\mathbf{g} - \boldsymbol{\mu}\|_2] \leq r$ , where  $0 \leq r \leq \|\boldsymbol{\mu}\|_2$ .

**Definition 2** ( $(r, m)$ - $L_1$  Byzantine resilience). Let  $\mathbf{g}^1, \dots, \mathbf{g}^{n-m}$  be independent identically distributed random vectors, where  $\mathbf{g}^i \in \mathbb{R}^d$ , and  $\mathbb{E}[\mathbf{g}^i] = \boldsymbol{\mu}$ . Let  $\mathbf{b}^1, \dots, \mathbf{b}^m$  be any random vectors in  $\mathbb{R}^d$ , possibly dependent on  $\mathbf{g}^i$ s. Aggregate rule  $\mathcal{A}$  is said to be  $(r, m)$ - $L_1$  Byzantine resilience if  $\mathbf{g} = \mathcal{A}(\mathbf{g}^1, \dots, \mathbf{g}^{n-m}, \mathbf{b}^1, \dots, \mathbf{b}^m)$  satisfies  $\mathbb{E}[\|\mathbf{g} - \boldsymbol{\mu}\|_1] \leq r$ , where  $0 \leq r \leq \|\boldsymbol{\mu}\|_1$ .

**Definition 3** (Sub-exponential random variable). A random variable  $X$  with  $\mathbb{E}[X] = \mu$  is called sub-exponential with parameters  $(v^2, \alpha)$  if  $\mathbb{E}[e^{\lambda(X-\mu)}] \leq e^{\frac{1}{2}v^2\lambda^2}, \forall |\lambda| < \frac{1}{\alpha}$ .

**Definition 4** (Gaussian random variable). A random variable  $X$  is Gaussian if  $X \sim \mathcal{N}(\mu, \sigma^2)$ , where  $\sim$  means “is of distribution”.

**Definition 5** (Lipschitz).  $h$  is  $L$ -Lipschitz if  $|h(\mathbf{w}) - h(\mathbf{w}')| \leq L\|\mathbf{w} - \mathbf{w}'\|_2, \forall \mathbf{w}, \mathbf{w}'$ .

**Definition 6** (Smoothness).  $h$  is  $L$ -smooth if  $|\nabla h(\mathbf{w}) - \nabla h(\mathbf{w}')| \leq L\|\mathbf{w} - \mathbf{w}'\|_2, \forall \mathbf{w}, \mathbf{w}'$ .

## 4 Methodology

In this section, we introduce the details of our FedRA. We first introduce the  $L_1$ -based Krum, which has a lower upper bound of error compared with the original Krum [4]. We then introduce our robust quantity-aware aggregation, which can filter malicious updates by jointly considering both updates and quantities. Finally, we propose a malicious client number estimator to dynamically determine the number of malicious clients in each round.

### 4.1 $L_1$ -based Krum

In this subsection, we introduce the  $L_1$ -based Krum, which changes the square distance in Krum [4] to  $L_1$  distance. More specifically, for the update of the  $i$ -th client  $\mathbf{g}^i$ , we first compute the  $L_1$  distance between  $\mathbf{g}^i$  and other  $(n-1)$  updates. For any  $j \neq i$ , we denote  $i \rightarrow j$  as the fact that  $\mathbf{g}^j$  belongs to the  $(n-m-2)$  updates closest to  $\mathbf{g}^i$  in terms of the  $L_1$  distance. Then we compute a score for  $\mathbf{g}^i$ , denoted as  $s(i) = \sum_{i \rightarrow j} \|\mathbf{g}^i - \mathbf{g}^j\|_1$ . Finally,  $L_1\text{-Krum}(\mathbf{g}^1, \dots, \mathbf{g}^n) = \mathbf{g}^{i_*}$ , where  $i_*$  refers to the client minimizing the score,  $s(i_*) \leq s(i), \forall i$ .

To prove that  $L_1$ -based Krum is Byzantine resilience, we follow Yin et al. [31] by assuming that the updates are all sub-exponential:

**Assumption 1** For any  $\mathbf{g}^i$ , its  $k$ -th dimension  $g_k^i$  is a sub-exponential variable with parameters  $(v_k^2, \alpha_k)$  where  $\mathbb{E}[g_k^i] = \mu_k, \mathbb{E}[(g_k^i - \mu_k)^2] = \sigma_k^2, v_k = \sigma_k$ , and  $\alpha_k < \frac{\sigma_k}{\sqrt{2 \ln 2n}}$ .

**Proposition 1** Let  $\mathbf{g}^1, \dots, \mathbf{g}^{n-m}$  be independently identically distributed updates, where  $\mathbf{g}^i \in \mathbb{R}^d$ , and  $\mathbb{E}[\mathbf{g}^i] = \boldsymbol{\mu}$ . Let  $\mathbf{b}^1, \dots, \mathbf{b}^m$  be any random vectors in  $\mathbb{R}^d$ , possibly dependent on  $\mathbf{g}^i$ s. Suppose that Assumption 1 holds for all benign updates. if  $2m+2 < n$  and  $\zeta(n, m)\|\boldsymbol{\sigma}\|_1 \leq \|\boldsymbol{\mu}\|_1$  where

$$\zeta(n, m) \stackrel{\text{def}}{=} \frac{3\sqrt{2 \ln 2}(n-m) + (n-2)\sqrt{2 \ln 2(n-m)}}{n-2m-2} = O(\sqrt{\ln n}) \quad (1)$$

and  $\boldsymbol{\sigma}$  is a  $d$ -dimensional vector denoted as  $[\sigma_1, \dots, \sigma_d]$ , then the  $L_1$ -based Krum is  $(r, m)$ - $L_1$  Byzantine resilience, where  $r = \zeta(n, m)\|\boldsymbol{\sigma}\|_1$ .

Proposition 1 is proved in Appendix A.1. It is obvious that the  $L_1$ -based Krum is also  $(r, m)$ -Byzantine resilience if  $\zeta(n, m)\|\boldsymbol{\sigma}\|_1 \leq \|\boldsymbol{\mu}\|_2$ . Compared with the error of the original square-distance-based Krum which is at least  $O(\sqrt{n})$ , the  $L_1$ -based Krum has a better expectation of error. Meanwhile, according to the experimental results shown in Appendix C.3, our  $L_1$ -based FedRA outperforms the variant using the square distance.

Following [31], we state the statistical error guarantees of the  $L_1$ -based Krum for strongly convex and smooth non-convex population loss function  $F$ .

**Assumption 2** (Smoothness of  $f$  and  $F$ ). For any  $z \in \mathcal{Z}$ , we assume that the partial derivative of  $f(\cdot; z)$  with respect to the  $k$ -th dimension of its first argument, denoted as  $\partial_k f(\cdot; z)$ , is  $L_k$ -Lipschitz for each  $k \in [1, d]$  and function  $f(\cdot; z)$  is  $L$ -smooth. We also assume that  $F(\cdot)$  is  $L_F$ -smooth. Let  $\hat{L} := (\sum_{k=1}^d L_k^2)^{\frac{1}{2}}$ . It is obvious that  $L_F \leq L \leq \hat{L}$ .

**Assumption 3** (Minimizer in  $\mathcal{W}$ ). Suppose that  $F(\mathbf{w})$  is  $\lambda_F$ -strongly convex, and let  $\mathbf{w}^* = \operatorname{argmin}_{\mathbf{w} \in \mathcal{W}} F(\mathbf{w})$ . We assume that  $\nabla F(\mathbf{w}^*) = 0$ .

**Theorem 1** Assume that Assumptions 1, 2 and 3 hold, and  $2m+2 < n$ . Choose  $\eta = 1/L_F$ . If  $\mathbf{w}_{t+1} = \mathbf{w}_t - \eta \mathbf{g}_t$ , after  $T$  iterations, we have

$$\mathbb{E}[\|\mathbf{w}_T - \mathbf{w}^*\|_2] \leq (1 - \frac{\lambda_F}{L_F + \lambda_F})^T \mathbb{E}[\|\mathbf{w}_0 - \mathbf{w}^*\|_2] + \frac{2}{\lambda_F} \zeta(n, m)\|\boldsymbol{\sigma}\|_1. \quad (2)$$

**Theorem 2** Assume that Assumptions 1 and 2 hold, and  $2m + 2 < n$ . Choose  $\eta = 1/L_F$ . If  $\mathbf{w}_{t+1} = \mathbf{w}_t - \eta \mathbf{g}_t$ , after  $T$  iterations, we have

$$\min_{t=0, \dots, T} \mathbb{E} [\|\nabla F(\mathbf{w}_t)\|_2^2] \leq \frac{2L_F}{T} \mathbb{E}[F(\mathbf{w}_0) - F(\mathbf{w}^*)] + (\zeta(n, m) \|\boldsymbol{\sigma}\|_1)^2. \quad (3)$$

Theorem 1 and 2 are proved in Appendices A.3 and A.4, respectively.

## 4.2 Robust Quantity-Aware Aggregation

In this subsection, we introduce our robust quantity-aware aggregation algorithm. The  $L_1$ -based Krum is a quantity-ignorant defense. We can intuitively improve the  $L_1$ -based Krum by selecting multiple updates and aggregating them with their quantities. We prove some propositions before introducing our intuition.

**Lemma 1** For any sample  $z \in \mathcal{Z}$ , suppose that  $\mathbb{E}[\partial_k f(\mathbf{w}; z)] = \mu_k$  and  $\mathbb{E}[(\partial_k f(\mathbf{w}; z) - \mu_k)^2] = \sigma_k^2$ , then for the update of the  $i$ -th benign client, we have  $\mathbb{E}[g_k^i] = \mu_k$  and  $\mathbb{E}[(g_k^i - \mu_k)^2] = \sigma_k^2/q^i$ .

Lemma 1 is proved in Appendix B.1. It indicates that the larger the quantity, the smaller the variance of an update. This explains why aggregations considering quantities have better performance. It also implies that an attacker can submit relatively low-variance updates and enlarge the quantity to amplify the impact of malicious updates to defeat quantity-aware defenses.

**Assumption 4** For any  $z \in \mathcal{Z}$ , the  $k$ -th dimension of  $\nabla f(\mathbf{w}; z)$  is a sub-exponential variable with parameters  $(v_k^2, \alpha_k)$  where  $\mathbb{E}[\partial_k f(\mathbf{w}; z)] = \mu_k$ ,  $\text{Var}(\partial_k f(\mathbf{w}; z)) = \sigma_k^2$ ,  $v_k = \sigma_k$ , and  $\alpha_k < \frac{\sigma_k}{\sqrt{2 \ln 2n}}$ .

**Assumption 5** For any  $z \in \mathcal{Z}$ , the  $k$ -th dimension of  $\nabla f(\mathbf{w}; z)$  is a Gaussian variable:  $\partial_k f(\mathbf{w}; z) \sim \mathcal{N}(\mu_k, \sigma_k^2)$ .

**Proposition 2** Let  $\mathbf{g}^i$  and  $\mathbf{g}^j$  be any pair of independently distributed benign updates and  $q^i$  and  $q^j$  be the corresponding quantities. Suppose that Assumption 4 holds, we then have

$$\mathbb{E} [\|\mathbf{g}^i - \mathbf{g}^j\|_1] \leq \sqrt{2 \ln 2} \sqrt{\frac{q^i + q^j}{q^i q^j}} \|\boldsymbol{\sigma}\|_1, \quad (4)$$

where  $\boldsymbol{\sigma}$  is a  $d$ -dimensional vector denoted as  $[\sigma_1, \dots, \sigma_d]$ .

**Proposition 3** Let  $\mathbf{g}^i$  and  $\mathbf{g}^j$  be any pair of independently distributed benign updates and  $q^i$  and  $q^j$  be the corresponding quantities. Suppose that Assumption 5 holds, we then have

$$\mathbb{E} [\|\mathbf{g}^i - \mathbf{g}^j\|_1] = \sqrt{\frac{2}{\pi}} \sqrt{\frac{q^i + q^j}{q^i q^j}} \|\boldsymbol{\sigma}\|_1, \quad (5)$$

where  $\boldsymbol{\sigma}$  is a  $d$ -dimensional vector denoted as  $[\sigma_1, \dots, \sigma_d]$ .

Propositions 2 and 3 are proved in Appendix B.2 and Appendix B.3, respectively. Define  $Q$  as:

$$Q(\mathbf{g}^i, \mathbf{g}^j, q^i, q^j) = \sqrt{\frac{q^i q^j}{q^i + q^j}} \|\mathbf{g}^i - \mathbf{g}^j\|_1. \quad (6)$$

---

### Algorithm 1 Robust Quantity-Aware Aggregation

---

**Input:**  $N, M, n, \{(\mathbf{g}_t^i, q_t^i) | i \in [n]\}$

- 1:  $\mathcal{S} \leftarrow \emptyset, m \leftarrow \lceil \frac{nM}{N} \rceil$
- 2: **for**  $i \in [n]$  **do**
- 3:      $s(i) \leftarrow (q^i)^\gamma \sum_{i \rightarrow j} Q(\mathbf{g}^i, \mathbf{g}^j, q^i, q^j)$
- 4:      $\mathcal{S} \leftarrow \mathcal{S} \cup \{s(i)\}$
- 5: **end for**
- $c \leftarrow \begin{cases} n - m - 1 & \text{fixed-ratio,} \\ n - MCNE(n, \mathcal{S}) & \text{dynamic-ratio.} \end{cases}$
- 6: selects  $c$  clients  $\mathcal{C}$  with smallest scores in  $\mathcal{S}$
- 7:  $\mathbf{g}_t \leftarrow \frac{1}{\sum_{i \in \mathcal{C}} q_t^i} \sum_{i \in \mathcal{C}} q_t^i \mathbf{g}_t^i$

---

From Propositions 2 and 3, we have  $\mathbb{E}[Q(\mathbf{g}^i, \mathbf{g}^j, q^i, q^j)] \leq \xi \|\boldsymbol{\sigma}\|_1$  when Assumption 4 or 5 holds, where  $\xi$  is a constant. It means that the upper bound of the value of  $\mathbb{E}[Q]$  is irrelevant with quantities. Based on  $Q$ , we modify the score of the  $i$ -th client in the  $L_1$ -based Krum to be

$$s(i) = \sum_{i \rightarrow j} Q(\mathbf{g}^i, \mathbf{g}^j, q^i, q^j), \quad (7)$$

where  $i \rightarrow j$  is defined in the first paragraph of Section 4.1. Finally, we select  $c$  clients with the smallest scores and compute the global update as  $\mathbf{g} = \frac{1}{\sum_{i \in \mathcal{C}} q^i} \sum_{i \in \mathcal{C}} q^i \mathbf{g}^i$ , where  $\mathcal{C}$  is the set of selected clients. In the fixed-ratio setting,  $c$  equals to  $n - \lceil \frac{nM}{N} \rceil - 1$  in each round.

However, only correcting the distance with  $Q$  is not enough. Suppose that the quantity of the  $i$ -th client is  $q^i$  and the  $k$ -th dimension of its updates is with variance  $\sigma_k^2/q^i$ . According to Lemma 1, the  $i$ -th client is likely to be benign. Assume that the learning rate is proportional to  $\sum_{i \in \mathcal{C}} q^i$ . If the update and quantity of the  $i$ -th client is selected, then it will add variance proportional to  $q^i \sigma_k^2$  into the  $k$ -th dimension of the final aggregated updates. Therefore, we further multiply the score by a penalty term. The final score is defined as

$$s(i) = (q^i)^\gamma \sum_{i \rightarrow j} Q(\mathbf{g}^i, \mathbf{g}^j, q^i, q^j), \quad (8)$$

where  $\gamma < 0.5$  is a hyper-parameter. The algorithm of our robust quantity-aware aggregation is shown in Algorithm 1.

### 4.3 Malicious Client Number Estimator

The above robust quantity-aware aggregation algorithm needs a parameter  $c$  to decide how many updates to be selected. In the fixed-ratio setting, we can set  $c = n - m - 1 = n - \lceil \frac{nM}{N} \rceil - 1$ . However, the number of malicious clients changes in different rounds in the dynamic-ratio setting. Setting  $c$  as the expectation of the number of benign clients in each round makes some malicious updates be definitely selected in some rounds, while setting  $c$  too small leads to a significant reduction in the amount of training data. Therefore, we propose a malicious client number estimator to predict the number of malicious clients in each round. Our malicious client estimator computes the number of malicious clients  $\tilde{m}$  by maximizing the log-likelihood as follows:

---

#### Algorithm 2 Malicious Client Number Estimator

---

**Input:**  $n, \{s(i) | i \in [n]\}$

**Output:**  $\tilde{m}$

- 1:  $\mathcal{L} \leftarrow \emptyset$
  - 2: **for**  $i = 0, 1, \dots, n$  **do**
  - 3:     Estimate  $\mu_b, \sigma_b, \mu_m, \sigma_m$  by Eq 12
  - 4:     Compute  $\hat{l}(i)$  through Eq 11
  - 5:      $\mathcal{L} \leftarrow \mathcal{L} \cup \{\hat{l}(i)\}$
  - 6: **end for**
  - 7:  $\tilde{m} \leftarrow \arg \max_{\tilde{m}} \mathcal{L}$
- 

$$\begin{aligned} \hat{l}(\tilde{m}) &= \ln p(\tilde{m}, s(1), \dots, s(n)) \\ &= \ln p(\tilde{m}) + \sum_{i=1}^n \ln p(s(i) | \tilde{m}). \end{aligned} \quad (9)$$

To simplify the problem, we assume the scores of benign and malicious clients follows two independent Gaussian distributions. Since  $\tilde{m}$  follows the hypergeometric distribution  $\mathcal{H}(n, M, N)$ , we have

$$\begin{aligned} \hat{l}(\tilde{m}) &= \ln \frac{\binom{M}{\tilde{m}} \binom{N-M}{n-\tilde{m}}}{\binom{N}{n}} - \sum_{i=1}^n \left( \ln \sigma_b \sqrt{2\pi} + \frac{(s(i) - \mu_b)^2}{2\sigma_b^2} \right) \mathbb{I}[i \notin \mathcal{M}] \\ &\quad - \sum_{i=1}^n \left( \ln \sigma_m \sqrt{2\pi} + \frac{(s(i) - \mu_m)^2}{2\sigma_m^2} \right) \mathbb{I}[i \in \mathcal{M}], \end{aligned} \quad (10)$$

where  $\mathbb{I}$  is the indicator function,  $\mathcal{M}$  is the estimated malicious clients set in the current round,  $|\mathcal{M}| = \tilde{m}$ ,  $\mu_b$  and  $\sigma_b^2$  are the mean and variance of benign scores, and  $\mu_m$  and  $\sigma_m^2$  are those of malicious scores. Suppose that our robust quantity-aware aggregation can effectively select malicious clients in the fixed-ratio settings, malicious clients will get the largest scores. We first sort the scores

by ascending order. Without loss of generality, we assume that the scores are already sorted, i.e.,  $s(i) < s(j), \forall i < j$ . Therefore, the Equation 10 can be simplified as

$$\hat{l}(\tilde{m}) \propto \ln \binom{M}{\tilde{m}} \binom{N-M}{n-\tilde{m}} - (n - \tilde{m}) \ln \sigma_b - \tilde{m} \ln \sigma_m - \sum_{i=1}^{n-\tilde{m}} \frac{(s(i) - \mu_b)^2}{2\sigma_b^2} - \sum_{i=n-\tilde{m}+1}^n \frac{(s(i) - \mu_m)^2}{2\sigma_m^2}. \quad (11)$$

The mean and variance of the two Gaussian distributions are estimated as follows:

$$\begin{aligned} \mu_b &= \frac{1}{n - \tilde{m}} \sum_{i=1}^{n-\tilde{m}} s(i), \quad \sigma_b^2 = \frac{1}{n - \tilde{m} - 1} \sum_{i=1}^{n-\tilde{m}} (s(i) - \mu_b)^2, \\ \mu_m &= \frac{1}{\tilde{m}} \sum_{i=n-\tilde{m}+1}^n s(i), \quad \sigma_m^2 = \frac{1}{\tilde{m} - 1} \sum_{i=n-\tilde{m}+1}^n (s(i) - \mu_m)^2. \end{aligned} \quad (12)$$

One may ask how  $s(i)$  is computed since it is relevant with  $\tilde{m}$ . A reasonable way is to initialize  $\tilde{m} = m = \lceil \frac{nM}{N} \rceil$ , iteratively compute  $s(i)$  and run the malicious client number estimator to update  $\tilde{m}$ . However, our experiments indicate that the performance without iterative approximation is already great enough. The algorithm of our malicious client number estimator is summarized in Algorithm 2.

## 5 Experiments

### 5.1 Datasets and Experimental Settings

**Dataset:** We conduct experiments on four public datasets: MNIST [11], CIFAR10 [10], Adult [5], and MIND [27]. We set the quantities of clients based on a long-tailed distribution, i.e., log-normal distribution. The average sample size of clients is around 20, and the  $\sigma$  of the log-normal distribution is 3. For the IID setting, we randomly shuffle the dataset and partition it according to the quantities. For the non-IID setting, we group the train samples according to their labels, and each client selects samples from a single group whenever possible. This guarantees that the local datasets of most clients contain only one class. The detailed dataset description and statistics are shown in Table 2.

**Configurations:** In our experiments, we use CNN networks as base models for the MNIST and CIFAR10 datasets. For the Adult dataset, we apply a three-layer feed-forward network as the base model. For the MIND dataset, we use a Text-CNN as the base model, and initialize the word embedding matrix with pre-trained Glove embeddings [16]. We apply FedAdam [21] to accelerate model convergence in all methods. We apply dropout with dropout rate 0.2 to mitigate over-fitting. The learning rate is 0.001 for CIFAR10 and Adult and 0.0001 for MNIST and MIND. The maximum of training rounds is 10,000 for MNIST and CIFAR10, 2,000 for Adult, and 15,000 for MIND. The ratio of malicious clients  $M/N$  is 0.1. The number of clients sampled in each round  $n$  is 50.  $\gamma$  is 0.1.

**Baselines:** We compare our FedRA with several baseline methods, including 1) Median [31], applying coordinate-wise median on each dimension of updates; 2) Trmean [31], applying coordinate-wise trimmed-mean on each dimension of updates; 3) Krum [4], selecting the update that is closest to a subset of neighboring updates based on the square distance; 4) mKrum [4], a variance of Krum that selects multiple updates and averages the selected updates; 5) Bulyan [6], selecting multiple clients with mKrum and aggregating the selected updates with Trmean; 6) Norm-bounding [25], clipping the  $L_2$  norm of each update with a certain threshold; 7) RFA [17], applying an approximation algorithm to minimize the geometric median of updates; 8) Truncate [18], limiting the quantity of each client under a dynamic threshold in each round and applying quantity-aware Trmean.

**Attack Model:** We suppose an attacker controls malicious clients. Each malicious client, if sampled, submits malicious updates and a malicious quantity. We implement three existing untargeted poisoning attack methods to create malicious updates, including 1) Label Flip [7]: a data poisoning attack that manipulates labels of training samples; 2) LIE [2]: adding small enough noise in updates to circumvent defenses; 3) Optimize [7]: a model poisoning attack that adds noise in the opposite position of benign updates. To create malicious quantities, the attacker first computes the mean and variance of benign quantities, which are denoted as  $\mu_q^m$  and  $\sigma_q^m$ , respectively. The malicious quantity is calculated as  $q = \mu_q^m + \alpha_q \sigma_q^m$ , where  $\alpha_q \in \{0, 1, 2, 5, 10\}$  is the quantity-enlarging factor.

Table 2: Dataset description and statistics.

Dataset	Task	#Classes	#Train	#Test	#Clients	#Train per client		
						Mean	Std	Max
MNIST	Image Classification	10	60,000	10,000	3,025	19.77	179.28	6,820
CIFAR10	Image Classification	10	50,000	10,000	3,115	16.05	200.14	8,933
Adult	Income Prediction	2	32,561	16,281	1,671	19.49	114.19	2,403
MIND	Text Classification	18	71,068	20,307	2,880	24.68	299.61	9,398

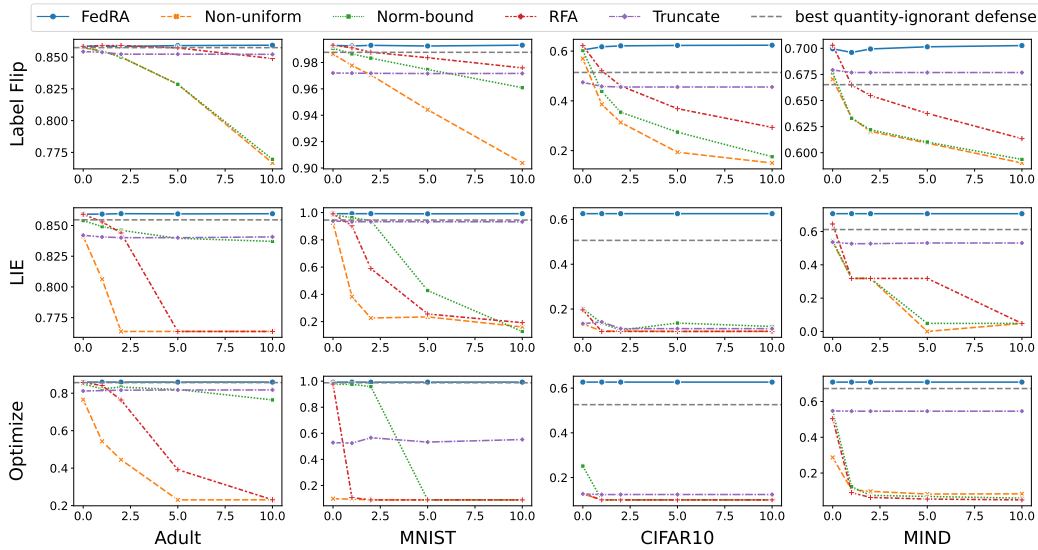


Figure 1: Performance comparison of defenses in the fixed-ratio IID setting. The x-axes are the values of accuracy. The y-axes are the values of quantity-enlarging factors.

## 5.2 Performance Evaluation in Fixed-ratio Setting

In this subsection, we conduct experiments in the fixed-ratio IID setting to analyze the effectiveness of our robust quantity-aware aggregation algorithm. The experimental results are shown in Figure 1. We can make the following observations from the figure. First, our FedRA outperforms the best quantity-ignorant defense in the fixed-ratio IID settings. This is because our method performs weighted averaging on selected updates based on their quantities. Second, our FedRA has stable performance with different quantity-enlarging factors. This is because FedRA can defend against quantity-enhanced attacks by jointly considering updates and quantities to filter malicious clients. These two observations reflect the effectiveness of our FedRA algorithm. Third, the performance of quantity-aware defenses, i.e., RFA and Norm-bound, becomes worse with larger quantity-enlarging factors. This is because these quantity-aware defenses by default treat received quantities as benign, which is vulnerable to quantity-enhanced attacks. Finally, Truncate has stable performance with different quantity-enlarging factors, but its performance is lower than FedRA. This is because the Truncate algorithm is quantity-robust by limiting quantities submitted by malicious clients. However, it also restricts quantities of benign clients. Meanwhile, it does not filter malicious clients by jointly considering quantities and updates. Thus, it has sub-optimal performance.

## 5.3 Performance Evaluation in Dynamic-ratio Setting

In this subsection, we conduct experiments in the dynamic-ratio IID setting to analyze the effectiveness of our malicious client number selector. The experimental results are shown in Figure 2. Besides the same observations in the fixed-ratio IID setting, we can make several additional observations. First, our FedRA has stable performance with different quantity-enlarging factors. It outperforms or has similar performance as the best quantity-ignorant defense. This shows the effectiveness of our FedRA with the malicious client estimator. Second, the algorithms that need the number or the upper bound of malicious clients, i.e., mKrum, Trmean, Bulyan, and Truncate, have lower performance in the dynamic-ratio IID setting than in the fixed-ratio IID setting. This is because these methods



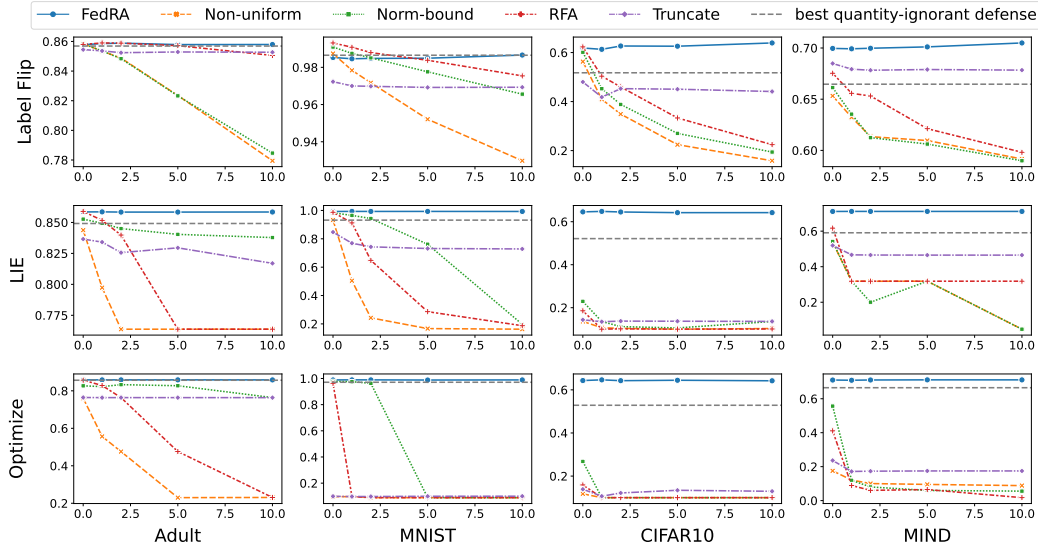


Figure 2: Performance of defenses in the dynamic-ratio IID setting. The x-axes are the values of accuracy. The y-axes are the values of quantity-enlarging factors.

definitely select malicious updates in some rounds in the dynamic-ratio setting. Finally, our FedRA with the malicious client estimator has lower performance in MNIST under the Label Flip attack. This may be because the scores in MNIST under the Label Flip attack do not follow two distant Gaussian distributions, which causes our malicious client number estimator to predict more than the actual number of malicious clients.

## 6 Discussion

**Performance in Non-IID setting.** We conduct experiments in the non-IID setting. The results are presented in Appendix C.2 due to limited space. The experimental results show that our FedRA still has great performance in most of the cases. However, unlike the IID setting, the performance in the Non-IID setting has no theoretical guarantees. Thus, it may fail in some cases, e.g., in Adult under the Label Flip attack in the fixed-ratio setting. We plan to improve our defense in Non-IID settings by combining with existing Federated Non-IID solutions [13, 24, 9].

**Performance with the malicious client estimator.** As shown in Section 5.3, our malicious client number estimator tends to select more malicious clients than expected because the scores may not follow two distant Gaussian distributions. We are studying a more effective malicious client number estimator without the assumption of two distant Gaussian distributions.

**Complexity.** The time complexity of FedRA is  $O(n^2d)$ , which is linear in the dimension of updates.

## 7 Conclusion

In this paper, we propose a robust aggregation method for federated learning, called FedRA. It aims to aggregate clients' local model updates with awareness of clients' quantities to benefit model performance while being quantity-robust to defend against quantity-enhanced attacks. We propose a method to filter malicious clients by jointly considering the uploaded model updates and data quantities from different clients, and perform quantity-aware weighted averaging on model updates from remaining clients. Since the number of malicious clients varies in different rounds, we further design a malicious client number estimator to determine the number of clients to be selected in each round. Experiments on four public datasets demonstrate the effectiveness of our FedRA and the malicious client number estimator.

## References

- [1] Eugene Bagdasaryan, Andreas Veit, Yiqing Hua, Deborah Estrin, and Vitaly Shmatikov. 2020. How to backdoor federated learning. In *AISTATS*. 2938–2948.
- [2] Gilad Baruch, Moran Baruch, and Yoav Goldberg. 2019. A Little Is Enough: Circumventing Defenses For Distributed Learning. In *NIPS*, Vol. 32.
- [3] Arjun Nitin Bhagoji, Supriyo Chakraborty, Prateek Mittal, and Seraphin Calo. 2019. Analyzing federated learning through an adversarial lens. In *ICML*. 634–643.
- [4] Peva Blanchard, El Mahdi El Mhamdi, Rachid Guerraoui, and Julien Stainer. 2017. Machine learning with adversaries: Byzantine tolerant gradient descent. *NIPS* 30 (2017).
- [5] Dheeru Dua and Casey Graff. 2017. UCI Machine Learning Repository. <http://archive.ics.uci.edu/ml>
- [6] El Mahdi El Mhamdi, Rachid Guerraoui, and Sébastien Rouault. 2018. The Hidden Vulnerability of Distributed Learning in Byzantium. In *ICML*, Vol. 80. 3521–3530.
- [7] Minghong Fang, Xiaoyu Cao, Jinyuan Jia, and Neil Zhenqiang Gong. 2020. Local Model Poisoning Attacks to Byzantine-Robust Federated Learning. In *USENIX*.
- [8] Andrew Hard, Kanishka Rao, Rajiv Mathews, Swaroop Ramaswamy, Françoise Beaufays, Sean Augenstein, Hubert Eichner, Chloé Kiddon, and Daniel Ramage. 2018. Federated learning for mobile keyboard prediction. *arXiv preprint arXiv:1811.03604* (2018).
- [9] Sai Praneeth Karimireddy, Satyen Kale, Mehryar Mohri, Sashank Reddi, Sebastian Stich, and Ananda Theertha Suresh. 2020. Scaffold: Stochastic controlled averaging for federated learning. In *ICML*. 5132–5143.
- [10] Alex Krizhevsky, Geoffrey Hinton, et al. 2009. Learning multiple layers of features from tiny images. (2009).
- [11] Yann LeCun, Léon Bottou, Yoshua Bengio, and Patrick Haffner. 1998. Gradient-based learning applied to document recognition. *Proc. IEEE* 86, 11 (1998), 2278–2324.
- [12] Jingjing Li, Ke Lu, Zi Huang, and Heng Tao Shen. 2017. Two Birds One Stone: On Both Cold-Start and Long-Tail Recommendation. In *MM*. 898–906.
- [13] Tian Li, Anit Kumar Sahu, Manzil Zaheer, Maziar Sanjabi, Ameet Talwalkar, and Virginia Smith. 2020. Federated optimization in heterogeneous networks. *Proceedings of Machine Learning and Systems 2* (2020), 429–450.
- [14] Yingqi Liu, Shiqing Ma, Yousra Aafer, Wen-Chuan Lee, Juan Zhai, Weihang Wang, and Xiangyu Zhang. 2017. Trojaning attack on neural networks. In *NDSS*.
- [15] Brendan McMahan, Eider Moore, Daniel Ramage, Seth Hampson, and Blaise Aguera y Arcas. 2017. Communication-efficient learning of deep networks from decentralized data. In *AISTATS*. 1273–1282.
- [16] Jeffrey Pennington, Richard Socher, and Christopher D Manning. 2014. Glove: Global vectors for word representation. In *EMNLP*. 1532–1543.
- [17] Krishna Pillutla, Sham M Kakade, and Zaid Harchaoui. 2019. Robust aggregation for federated learning. *arXiv preprint arXiv:1912.13445* (2019).
- [18] Amit Portnoy, Yoav Tirosh, and Danny Hendler. 2020. Towards Federated Learning With Byzantine-Robust Client Weighting. *arXiv preprint arXiv:2004.04986* (2020).
- [19] Tao Qi, Fangzhao Wu, Chuhan Wu, Yongfeng Huang, and Xing Xie. 2020. Privacy-Preserving News Recommendation Model Learning. In *Findings of EMNLP*. 1423–1432.
- [20] Tao Qi, Fangzhao Wu, Chuhan Wu, Yongfeng Huang, and Xing Xie. 2021. Uni-FedRec: A Unified Privacy-Preserving News Recommendation Framework for Model Training and Online Serving. In *Findings of EMNLP*. 1438–1448.

- [21] Sashank J. Reddi, Zachary Charles, Manzil Zaheer, Zachary Garrett, Keith Rush, Jakub Konečný, Sanjiv Kumar, and Hugh Brendan McMahan. 2021. Adaptive Federated Optimization. In *ICLR*.
- [22] Nicola Rieke, Jonny Hancox, Wenqi Li, Fausto Milletari, Holger R Roth, Shadi Albarqouni, Spyridon Bakas, Mathieu N Galtier, Bennett A Landman, Klaus Maier-Hein, et al. 2020. The future of digital health with federated learning. *NPJ digital medicine* 3, 1 (2020), 1–7.
- [23] Micah J Sheller, Brandon Edwards, G Anthony Reina, Jason Martin, Sarthak Pati, Aikaterini Kotrotsou, Mikhail Milchenko, Weilin Xu, Daniel Marcus, Rivka R Colen, et al. 2020. Federated learning in medicine: facilitating multi-institutional collaborations without sharing patient data. *Scientific reports* 10, 1 (2020), 1–12.
- [24] Virginia Smith, Chao-Kai Chiang, Maziar Sanjabi, and Ameet S Talwalkar. 2017. Federated multi-task learning. *NIPS* 30 (2017).
- [25] Ziteng Sun, Peter Kairouz, Ananda Theertha Suresh, and H Brendan McMahan. 2019. Can you really backdoor federated learning? *arXiv preprint arXiv:1911.07963* (2019).
- [26] Hongyi Wang, Kartik Sreenivasan, Shashank Rajput, Harit Vishwakarma, Saurabh Agarwal, Jyong Sohn, Kangwook Lee, and Dimitris S. Papailiopoulos. 2020. Attack of the Tails: Yes, You Really Can Backdoor Federated Learning. In *NIPS*.
- [27] Fangzhao Wu, Ying Qiao, Jiun-Hung Chen, Chuhan Wu, Tao Qi, Jianxun Lian, Danyang Liu, Xing Xie, Jianfeng Gao, Winnie Wu, and Ming Zhou. 2020. MIND: A Large-scale Dataset for News Recommendation. In *ACL*. 3597–3606.
- [28] Chulin Xie, Keli Huang, Pin-Yu Chen, and Bo Li. 2020. DBA: Distributed Backdoor Attacks against Federated Learning. In *ICLR*.
- [29] Timothy Yang, Galen Andrew, Hubert Eichner, Haicheng Sun, Wei Li, Nicholas Kong, Daniel Ramage, and Françoise Beaufays. 2018. Applied federated learning: Improving google keyboard query suggestions. *arXiv preprint arXiv:1812.02903* (2018).
- [30] Jingwei Yi, Fangzhao Wu, Chuhan Wu, Ruixuan Liu, Guangzhong Sun, and Xing Xie. 2021. Efficient-FedRec: Efficient Federated Learning Framework for Privacy-Preserving News Recommendation. In *EMNLP*. 2814–2824.
- [31] Dong Yin, Yudong Chen, Ramchandran Kannan, and Peter Bartlett. 2018. Byzantine-robust distributed learning: Towards optimal statistical rates. In *ICML*. 5650–5659.
- [32] Manzil Zaheer, Sashank Reddi, Devendra Sachan, Satyen Kale, and Sanjiv Kumar. 2018. Adaptive methods for nonconvex optimization. *NIPS* 31 (2018).
- [33] Xiao Zhang, Zhiyuan Fang, Yandong Wen, Zhifeng Li, and Yu Qiao. 2017. Range Loss for Deep Face Recognition With Long-Tailed Training Data. In *ICCV*. 5419–5428.
- [34] Yaoyao Zhong, Weihong Deng, Mei Wang, Jiani Hu, Jianteng Peng, Xunqiang Tao, and Yaohai Huang. 2019. Unequal-Training for Deep Face Recognition With Long-Tailed Noisy Data. In *CVPR*. 7804–7813.

## Supplementary Material

### A L1-based Krum

#### A.1 Proof of Proposition 1

*Proof.* Without loss of generality, we assume malicious vectors are placed in the last  $m$  positions in the arguments of the  $L_1$ -based Krum, i.e.,  $\mathbf{g} = L_1\text{-Krum}(\mathbf{g}^1, \dots, \mathbf{g}^{n-m}, \mathbf{b}^1, \dots, \mathbf{b}^m)$ . For each index  $i$ , we denote the number of benign indexes  $j$  such that  $i \rightarrow j$  as  $\delta_c(i)$ , and the number of malicious indexes  $j$  such that  $i \rightarrow j$  as  $\delta_b(i)$ . We have

$$\begin{aligned} \delta_c(i) + \delta_b(i) &= n - m - 2, \\ n - 2m - 2 &\leq \delta_c(i) \leq n - m - 2, \\ \delta_b(i) &\leq m. \end{aligned} \tag{1}$$

We denote the  $i_*$  as the index selected by  $L_1$ -Krum.

$$\begin{aligned} \mathbb{E}[\|\mathbf{g} - \boldsymbol{\mu}\|_1] &\leq \sum_{\text{correct } i} \mathbb{E}[\|\mathbf{g}^i - \boldsymbol{\mu}\|_1 \mathbb{I}(i_* = i)] \\ &\quad + \sum_{\text{malicious } k} \mathbb{E}[\|\mathbf{b}^k - \boldsymbol{\mu}\|_1 \mathbb{I}(i_* = k)], \end{aligned} \tag{2}$$

where  $\mathbb{I}$  denotes the indicator function. We focus on the case that  $i_* = i$  for some correct index  $i$  in Equation 2. We first prove the following lemma.

**Lemma 2** *Let  $\mathbf{g}^1, \dots, \mathbf{g}^n$  be independent identically distributed random vectors, where  $\mathbf{g}^i \subseteq \mathbb{R}^d$ , and  $\mathbb{E}[\mathbf{g}^i] = \boldsymbol{\mu}$ . Supposing that Assumption 1 holds, then we have*

$$\mathbb{E}[\max_i \|\mathbf{g}^i - \boldsymbol{\mu}\|_1] \leq \sqrt{2 \ln 2n} \|\boldsymbol{\sigma}\|_1, \tag{3}$$

where  $\boldsymbol{\sigma}$  is a  $d$ -dimensional vector denoted as  $[\sigma_1, \dots, \sigma_d]$ .

*Proof.* See Appendix A.2.

Applying Lemma 2 on the first term of Equation 2, we obtain

$$\begin{aligned} \sum_{\text{correct } i} \mathbb{E}[\|\mathbf{g}^i - \boldsymbol{\mu}\|_1 \mathbb{I}(i_* = i)] &\leq \mathbb{E}[\max_{\text{correct } i} \|\mathbf{g}^i - \boldsymbol{\mu}\|_1] \\ &\leq \sqrt{2 \ln 2(n-m)} \|\boldsymbol{\sigma}\|_1. \end{aligned} \tag{4}$$

Next we focus on the case that  $i_* = k$  for some malicious index  $k$  in Equation 2.

$$\begin{aligned} &\sum_{\text{malicious } k} \mathbb{E}[\|\mathbf{b}^k - \boldsymbol{\mu}\|_1 \mathbb{I}(i_* = k)] \\ &\leq \sum_{\text{malicious } k} \mathbb{E}[\|\boldsymbol{\mu} - \frac{1}{\delta_c(k)} \sum_{k \rightarrow \text{correct } j} \mathbf{g}^j\|_1 \mathbb{I}(i_* = k)] \\ &\quad + \sum_{\text{malicious } k} \mathbb{E}[\|\mathbf{b}^k - \frac{1}{\delta_c(k)} \sum_{k \rightarrow \text{correct } j} \mathbf{g}^j\|_1 \mathbb{I}(i_* = k)] \\ &\leq \mathbb{E}[\max_{\text{malicious } k} \frac{1}{\delta_c(k)} \sum_{\text{correct } j} \|\boldsymbol{\mu} - \mathbf{g}^j\|_1] \\ &\quad + \sum_{\text{malicious } k} \mathbb{E}[\|\mathbf{b}^k - \frac{1}{\delta_c(k)} \sum_{k \rightarrow \text{correct } j} \mathbf{g}^j\|_1 \mathbb{I}(i_* = k)] \end{aligned} \tag{5}$$

If  $k$  is selected by the  $L_1$ -based Krum, it implies for any correct index  $i$

$$\begin{aligned} &\sum_{\text{malicious } k} \mathbb{I}(i_* = k) [\sum_{k \rightarrow \text{correct } j} \|\mathbf{b}^k - \mathbf{g}^j\|_1 + \sum_{k \rightarrow \text{malicious } j} \|\mathbf{b}^k - \mathbf{b}^j\|_1] \\ &\leq \sum_{i \rightarrow \text{correct } j} \|\mathbf{g}^i - \mathbf{g}^j\|_1 + \sum_{i \rightarrow \text{malicious } j} \|\mathbf{g}^i - \mathbf{b}^j\|_1. \end{aligned} \tag{6}$$

Therefore, for any correct index  $i$

$$\begin{aligned}
& \sum_{\text{malicious } k} \left\| \mathbf{b}^k - \frac{1}{\delta_c(k)} \sum_{k \rightarrow \text{correct } j} \mathbf{g}^j \right\|_1 \mathbb{I}(i_* = k) \\
& \leq \sum_{\text{malicious } k} \frac{\mathbb{I}(i_* = k)}{\delta_c(k)} \sum_{k \rightarrow \text{correct } j} \|\mathbf{b}^k - \mathbf{g}^j\|_1 \\
& \leq \frac{1}{n - 2m - 2} \sum_{i \rightarrow \text{correct } j} \|\mathbf{g}^i - \mathbf{g}^j\|_1 + \frac{1}{n - 2m - 2} \sum_{i \rightarrow \text{malicious } j} \|\mathbf{g}^i - \mathbf{b}^j\|_1.
\end{aligned} \tag{7}$$

We focus on the second term of Equation 7. Since any correct index  $i$  has  $n - m - 2$  neighbors and  $f + 1$  non-neighbors. There exists at least one benign index  $\zeta(i)$ , which is farther from  $i$  than any of its neighbors. Therefore,  $\forall i \rightarrow \text{malicious } j$ ,  $\|\mathbf{g}^i - \mathbf{b}^j\|_1 \leq \|\mathbf{g}^i - \mathbf{g}^{\zeta(i)}\|_1$ . Then we have

$$\begin{aligned}
& \sum_{\text{malicious } k} \left\| \mathbf{b}^k - \frac{1}{\delta_c(k)} \sum_{k \rightarrow \text{correct } j} \mathbf{g}^j \right\|_1 \mathbb{I}(i_* = k) \\
& \leq \frac{1}{n - 2m - 2} \sum_{i \rightarrow \text{correct } j} \|\mathbf{g}^i - \mathbf{g}^j\|_1 + \frac{\delta_b(i)}{n - 2m - 2} \|\mathbf{g}^i - \mathbf{g}^{\zeta(i)}\|_1.
\end{aligned} \tag{8}$$

$$\begin{aligned}
& \sum_{\text{malicious } k} \mathbb{E} \left[ \left\| \mathbf{b}^k - \frac{1}{\delta_c(k)} \sum_{k \rightarrow \text{correct } j} \mathbf{g}^j \right\|_1 \mathbb{I}(i_* = k) \right] \\
& \leq \frac{2\sqrt{2 \ln 2} (n - m)}{n - 2m - 2} \|\boldsymbol{\sigma}\|_1 + \frac{\delta_b(i)}{n - 2m - 2} \sum_{\text{correct } j \neq i} \mathbb{E} [\|\mathbf{g}^i - \mathbf{g}^j\|_1 \mathbb{I}(\zeta(i) = j)] \\
& \leq \frac{2\sqrt{2 \ln 2} (n - m)}{n - 2m - 2} \|\boldsymbol{\sigma}\|_1 + \frac{\delta_b(i)}{n - 2m - 2} \mathbb{E} \max_{\text{correct } j \neq i} \|\mathbf{g}^i - \mathbf{g}^j\|_1 \\
& \leq \frac{2\sqrt{2 \ln 2} (n - m) + 2m\sqrt{2 \ln 2} (n - m)}{n - 2m - 2} \|\boldsymbol{\sigma}\|_1.
\end{aligned} \tag{9}$$

Putting Equation 9 back to Equation 5, we obtain

$$\sum_{\text{malicious } k} \mathbb{E} [\|\mathbf{b}^k - \boldsymbol{\mu}\|_1 \mathbb{I}(i_* = k)] \leq \frac{3\sqrt{2 \ln 2} (n - m) + 2m\sqrt{2 \ln 2} (n - m)}{n - 2m - 2} \|\boldsymbol{\sigma}\|_1 \tag{10}$$

Putting everything back together, we get

$$\mathbb{E} [\|\mathbf{g} - \boldsymbol{\mu}\|_1] \leq \frac{3\sqrt{2 \ln 2} (n - m) + (n - 2)\sqrt{2 \ln 2} (n - m)}{n - 2m - 2} \|\boldsymbol{\sigma}\|_1. \tag{11}$$

## A.2 Proof of Lemma 2

*Proof.* We first convert the problem of computing the expectation of the maximum of the  $L_1$  norm of the  $d$ -dimensional vectors into the problem of computing expectations of the maximum of each dimension of the  $d$ -dimensional vectors.

$$\begin{aligned}
\mathbb{E} [\max_i \|\mathbf{g}^i - \boldsymbol{\mu}\|_1] &= \mathbb{E} [\max_i \sum_{k \in \{1, \dots, d\}} |g_k^i - \mu_k|] \\
&\leq \sum_{k \in \{1, \dots, d\}} \mathbb{E} [\max_i |g_k^i - \mu_k|].
\end{aligned} \tag{12}$$

Define  $x_k^i = g_k^i - \mu_k$ . Denote a list of values  $X = \{x_k^1, -x_k^1, \dots, x_k^n, -x_k^n\}$ , and  $z_k = \max_i |g_k^i - \mu_k| = \max_{x \in X} x$ . We then obtain

$$\begin{aligned}
e^{\lambda \mathbb{E}[z_k]} &\leq \mathbb{E}[e^{\lambda z_k}] \text{ (Jensen inequality)} \\
&= \mathbb{E} [\max_{x \in X} e^{\lambda x}] \leq \sum_{x \in X} \mathbb{E}[e^{\lambda x}] \leq 2ne^{\frac{\lambda^2 \sigma_k^2}{2}} \text{ (Assumption 1)}.
\end{aligned} \tag{13}$$

$$\mathbb{E}[z_k] \leq \frac{\ln 2n}{\lambda} + \frac{\lambda\sigma_k^2}{2}. \quad (14)$$

Setting  $\lambda = \frac{\sqrt{2\ln 2n}}{\sigma_k} < \frac{1}{\alpha}$ , we can get

$$\mathbb{E}[z_k] \leq \sigma_k \sqrt{2\ln 2n}. \quad (15)$$

Putting Equation 15 back to Equation 12, we obtain

$$\mathbb{E}[\max_i \|\mathbf{g}^i - \boldsymbol{\mu}\|_1] \leq \sqrt{2\ln 2n} \|\boldsymbol{\sigma}\|_1, \quad (16)$$

where  $\boldsymbol{\sigma}$  is a d-dimensional vector denoted as  $[\sigma_1, \dots, \sigma_d]$ .

### A.3 Proof of Theorem 1

*Proof.* According to the proof of Theorem 1 in [31], if  $F(\mathbf{w})$  is  $\lambda_F$ -strongly convex, we have

$$\|\mathbf{w}_t - \eta \nabla F(\mathbf{w}_t) - \mathbf{w}^*\|_2 \leq \left(1 - \frac{\lambda_F}{L_F + \lambda_F}\right) \|\mathbf{w}_t - \mathbf{w}^*\|_2. \quad (17)$$

We further have

$$\begin{aligned} \|\mathbf{w}_{t+1} - \mathbf{w}^*\|_2 &\leq \|\mathbf{w}_t - \eta \nabla F(\mathbf{w}^*) - \mathbf{w}^*\|_2 + \eta \|\mathbf{g}_t - \nabla F(\mathbf{w}_t)\|_2 \\ &\leq \left(1 - \frac{\lambda_F}{L_F + \lambda_F}\right) \|\mathbf{w}_t - \mathbf{w}^*\|_2 + \eta \|\mathbf{g}_t - \nabla F(\mathbf{w}_t)\|_1. \end{aligned} \quad (18)$$

When we set  $\eta = \frac{1}{L_F}$ , according to Proposition 1, we obtain

$$\mathbb{E}[\|\mathbf{w}_{t+1} - \mathbf{w}^*\|_2] \leq \left(1 - \frac{\lambda_F}{L_F + \lambda_F}\right) \mathbb{E}[\|\mathbf{w}_t - \mathbf{w}^*\|_2] + \frac{1}{L_F} \zeta(n, m) \|\boldsymbol{\sigma}\|_1, \quad (19)$$

where

$$\zeta(n, m) = \frac{3\sqrt{2\ln 2}(n-m) + (n-2)\sqrt{2\ln 2(n-m)}}{n-2m-2}. \quad (20)$$

Iterating Equation 19, we have

$$\mathbb{E}[\|\mathbf{w}_T - \mathbf{w}^*\|_2] \leq \left(1 - \frac{\lambda_F}{L_F + \lambda_F}\right)^T \mathbb{E}[\|\mathbf{w}_0 - \mathbf{w}^*\|_2] + \frac{2}{\lambda_F} \zeta(n, m) \|\boldsymbol{\sigma}\|_1. \quad (21)$$

### A.4 Proof of Theorem 2

*Proof.* Following the proof of Theorem 2 in [31], using the smoothness of  $F(\cdot)$  and setting  $\eta = 1/L_F$ , we have

$$F(\mathbf{w}_{t+1}) \leq F(\mathbf{w}_t) - \frac{1}{2L_F} \|\nabla F(\mathbf{w}_t)\|_2^2 + \frac{1}{2L_F} \|\mathbf{g}_t - \nabla F(\mathbf{w}_t)\|_2^2. \quad (22)$$

According to Proposition 1, we further obtain

$$\mathbb{E}[F(\mathbf{w}_{t+1}) - F(\mathbf{w}^*)] \leq \mathbb{E}[F(\mathbf{w}_t) - F(\mathbf{w}^*)] - \frac{1}{2L_F} \mathbb{E}[\|\nabla F(\mathbf{w}_t)\|_2^2] + \frac{1}{2L_F} (\zeta(n, m) \|\boldsymbol{\sigma}\|_1)^2. \quad (23)$$

Sum up Equation 23, we have

$$\begin{aligned} 0 &\leq \mathbb{E}[F(\mathbf{w}_T) - F(\mathbf{w}^*)] \\ &\leq \mathbb{E}[F(\mathbf{w}^0) - F(\mathbf{w}^*)] - \frac{1}{2L_F} \sum_{t=0}^{T-1} \mathbb{E}[\|\nabla F(\mathbf{w}_t)\|_2^2] + \frac{T}{2L_F} (\zeta(n, m) \|\boldsymbol{\sigma}\|_1)^2, \end{aligned} \quad (24)$$

which implies

$$\min_{t=0, \dots, T} \mathbb{E}[\|\nabla F(\mathbf{w}_t)\|_2^2] \leq \frac{2L_F}{T} \mathbb{E}[F(\mathbf{w}_0) - F(\mathbf{w}^*)] + (\zeta(n, m) \|\boldsymbol{\sigma}\|_1)^2. \quad (25)$$

## B Quantity-aware Robust Aggregation

### B.1 Proof of Lemma 1

*Proof.* As defined in Section 3, we have  $g_k^i = \frac{1}{q_i} \sum_{z \in \mathcal{D}_i} \partial_k f(\mathbf{w}; z)$ . Therefore, we can obtain

$$\mathbb{E}[g_k^i] = \frac{1}{q_i} \sum_{z \in \mathcal{D}_i} \mathbb{E}[\partial_k f(\mathbf{w}; z)] = \mu_k, \quad (26)$$

$$\begin{aligned} \mathbb{E}[(g_k^i - \mu_k)^2] &= \mathbb{E}\left[\left(\frac{1}{q_i} \sum_{z \in \mathcal{D}_i} \partial_k f(\mathbf{w}; z) - \mu_k\right)^2\right] \\ &= \frac{1}{q_i^2} \sum_{z \in \mathcal{D}_i} \mathbb{E}[(\partial_k f(\mathbf{w}; z) - \mu_k)^2] = \frac{\sigma_k^2}{q_i}. \end{aligned} \quad (27)$$

### B.2 Proof of Proposition 2

*Proof.* Similar to Appendix A.2, We first convert the problem into computing expectations of each dimension.

$$\begin{aligned} \mathbb{E}[\|\mathbf{g}^i - \mathbf{g}^j\|_1] &= \mathbb{E}\left[\sum_{k \in \{1, \dots, d\}} |g_k^i - g_k^j|\right] \\ &= \sum_{k \in \{1, \dots, d\}} \mathbb{E}[|g_k^i - g_k^j|]. \end{aligned} \quad (28)$$

Since any  $z \in \mathcal{D}_i$  are independent, if  $|\lambda| < \frac{q^i}{\alpha_k}$ , we then have

$$\mathbb{E}[e^{\lambda(g_k^i - \mu_k)}] = \mathbb{E}[e^{\frac{\lambda}{q^i} \sum_{z \in \mathcal{D}_i} (\partial_k f(\mathbf{w}; z) - \mu_k)}] \leq e^{\frac{\lambda^2 \sigma_k^2}{2q^i}}, \quad (29)$$

which implies  $g_k^i$  is sub-exponential with parameters  $(\frac{\sigma_k^2}{q^i}, \frac{\alpha_k}{q^i})$ , where  $\alpha_k < \frac{\sigma_k}{\sqrt{2 \ln 2n}}$ .

Let  $|\lambda| < \min(\frac{q^i}{\alpha_k}, \frac{q^j}{\alpha_k})$ . Since  $g_k^i$  and  $g_k^j$  are independently distributed, we can obtain

$$\begin{aligned} \mathbb{E}[e^{\lambda(g_k^i - g_k^j)}] &= \mathbb{E}[e^{\lambda((g_k^i - \mu_k) - (g_k^j - \mu_k))}] \\ &= \mathbb{E}[e^{\lambda(g_k^i - \mu_k)}] \mathbb{E}[e^{-\lambda(g_k^j - \mu_k)}] \\ &\leq e^{\frac{\lambda^2 \sigma_k^2}{2} \frac{q^i + q^j}{q^i q^j}}. \end{aligned} \quad (30)$$

Then following similar steps in Appendix A.2 and setting  $\lambda = \frac{\sqrt{2 \ln 2n}}{\sigma_k} \sqrt{\frac{q^i q^j}{q^i + q^j}}$ , we can have

$$\mathbb{E}[\|\mathbf{g}^i - \mathbf{g}^j\|_1] \leq \sqrt{2 \ln 2} \|\boldsymbol{\sigma}\|_1 \sqrt{\frac{q^i + q^j}{q^i q^j}}. \quad (31)$$

### B.3 Proof of Proposition 3

Following Appendix B.2, we compute the expectation of each dimension first. It is obvious that  $(g_k^i - g_k^j) \sim \mathcal{N}(0, \frac{q^i + q^j}{q^i q^j} \sigma_k^2)$ . Denoting  $\sigma_k'^2 = \frac{q^i + q^j}{q^i q^j} \sigma_k^2$  and  $x = g_k^i - g_k^j$ , we then have

$$\mathbb{E}[|x|] = \int_{-\infty}^{\infty} |x| \frac{1}{\sigma_k'^2 \sqrt{2\pi}} e^{-\frac{x^2}{2\sigma_k'^2}} dx = \sqrt{\frac{2}{\pi}} \sigma_k'. \quad (32)$$

Therefore, we can get

$$\mathbb{E}[\|\mathbf{g}^i - \mathbf{g}^j\|_1] = \sqrt{\frac{2}{\pi}} \sqrt{\frac{q^i + q^j}{q^i q^j}} \|\boldsymbol{\sigma}\|_1. \quad (33)$$

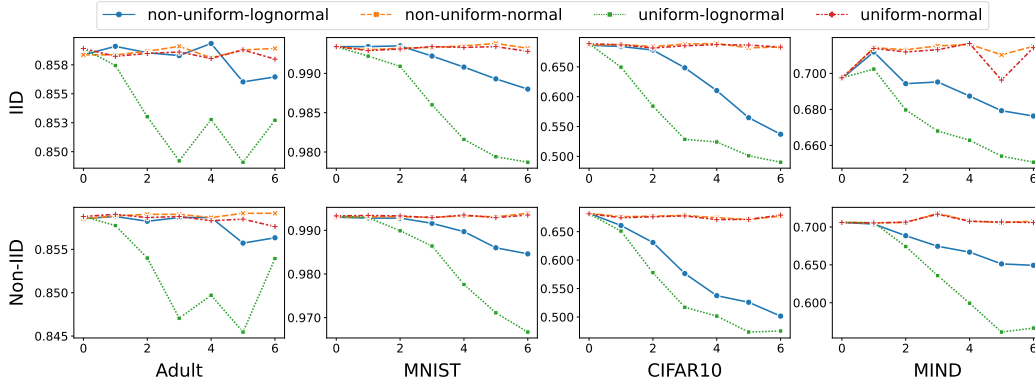


Figure 3: Performance of non-uniform and uniform aggregation in different data distributions. The x-axes are the values of accuracy. The y-axes are the values of  $\sigma$  in the Gaussian distributions or the log-normal distributions.

Table 3: Performance of different existing defense methods without attacks.

		Uniform	Median	Tmean	Krum	mKrum	Bulyan	Non-uniform	Norm-bound	RFA
IID	Adult	0.8492	0.8171	0.8548	0.8318	0.8517	0.8546	0.8583	0.8587	0.8581
	MNIST	0.9878	0.8744	0.9876	0.8656	0.9885	0.9881	0.9933	0.9935	0.9927
	CIFAR10	0.5322	0.3451	0.5515	0.5376	0.5351	0.5545	0.6488	0.6525	0.6454
	MIND	0.6700	0.6476	0.6825	0.6147	0.6712	0.6818	0.6948	0.6945	0.6927
non-IID	Adult	0.8471	0.7638	0.8512	0.7638	0.8521	0.8541	0.8587	0.8585	0.8569
	MNIST	0.9864	0.4478	0.9866	0.3470	0.9883	0.9872	0.9922	0.9915	0.9905
	CIFAR10	0.5224	0.1930	0.5397	0.2058	0.5335	0.5407	0.5771	0.5773	0.5547
	MIND	0.6293	0.5745	0.6105	0.5435	0.6386	0.6251	0.6815	0.6760	0.6761

## C Additional Experiment

### C.1 Importance of Quantity

In this subsection, we state the importance of quantity. We first analyze which factors influence the impact of quantities. We introduce non-uniform aggregation as performing weighted averaging on updates according to client quantities, while uniform aggregation as averaging updates without considering quantities. It is obvious that when all benign clients have same quantities, it is unnecessary to apply non-uniform aggregation. Meanwhile, we find non-uniform aggregation does not always significantly outperform uniform aggregation in some datasets (Table 4 on MIND<sup>1</sup>, Table 6 on LEAF<sup>2</sup>, and Table 5 on ML-1M<sup>3</sup>). We conduct experiments to study the impact of

- Skewness: We sample the clients’ quantities from Gaussian distributions and log-normal distributions, respectively, and set the average quantity as 20.
- Variance: We vary the  $\sigma$  of the Gaussian distributions and the log-normal distributions. Higher  $\sigma$  means higher variance of clients’ quantities.
- non-IID: For the IID setting, we randomly divide dataset into clients local datasets. For the non-IID setting, we guarantee the local datasets of most clients contain only one class.

The experimental results are shown in Figure 3, wherein we can make several observations. First, when client quantities are sampled from log-normal distributions, the performance difference of the uniform aggregation and the non-uniform aggregation are more significant. It shows that skewness is one of the important factors. Second, under the log-normal settings, when we enlarge the variance of quantities, the performance difference becomes larger. It shows that variance is another important factor. Finally, comparing the IID and non-IID settings, the performance difference does not change, which shows that non-IID is not an important factor. Since the log-normal distribution is a log-tailed

<sup>1</sup><https://msnews.github.io/>

<sup>2</sup><https://leaf.cmu.edu/>

<sup>3</sup><https://grouplens.org/datasets/movielens/>



Table 6: Performance on LEAF.

	FEMNIST	CelabA	Shakespeare	Reddit
Non-uniform	80.19	87.16	47.80	11.73
Uniform	80.01	87.52	47.97	11.68

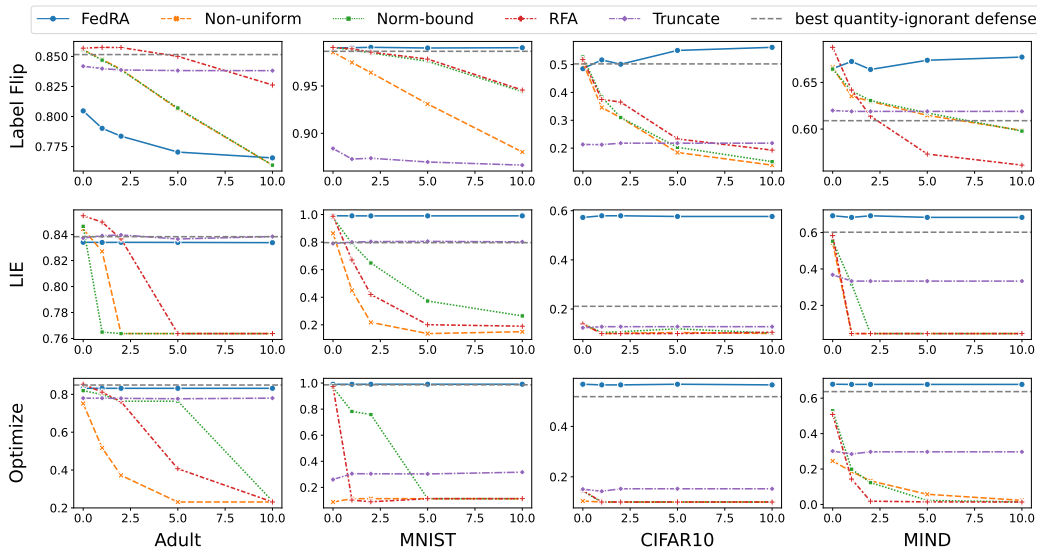


Figure 4: Performance of defenses in the fixed-ratio non-IID setting. The x-axes are the values of accuracy. The y-axes are the values of quantity-enlarging factors.

distribution, which is common in real-world scenarios and has been widely researched, we think it is necessary to study the robustness of federated learning under this setting.

Table 4: Performance of recommendation on MIND.

	AUC	MRR	nDCG@5	nDCG@10
Non-uniform	66.56	31.40	34.69	41.05
Uniform	64.24	29.88	32.56	39.10

Table 5: Performance on ML-1M.

	Hit@10	nDCG@10
Non-uniform	67.12	38.32
Uniform	59.00	32.48

We further test the performance of different existing defense methods without attacks under the log-normal distribution with  $\sigma = 3.0$ . The experimental results are shown in Table 3. The quantity-ignored defenses have lower performance than the quantity-aware defenses on the four datasets, which shows the importance of quantity.

## C.2 Performance Evaluation in Non-IID setting

In this subsection, we first conduct experiments in the fixed-ratio non-IID setting. The results are shown in Figure 4. We can observe that the performance of our FedRA is stable with quantity-enlarging factors except in Adult under Label Flip attacks. The performance of FedRA is higher than that of the best quantity-ignorant defense except for the Adult dataset. It might be because the defense in the Adult dataset is more sensitive with the non-IID setting. We then conduct experiments in the dynamic-ratio non-IID setting. The results are shown in Figure 5. The performance of our FedRA is stable with the quantity-enlarging factors and higher than that of the best quantity-ignorant defense except those with the Label-Flip attack. It might be because the quantity-robust scores may not follow two distant Gaussian distributions that we have assumed. Overall, our method does not have a theoretical guarantee for non-IID settings, and the above results empirically prove that our FedRA can have great performance in most of the non-IID settings. We will improve our method in the future as we discussed in Section 6 of the paper.

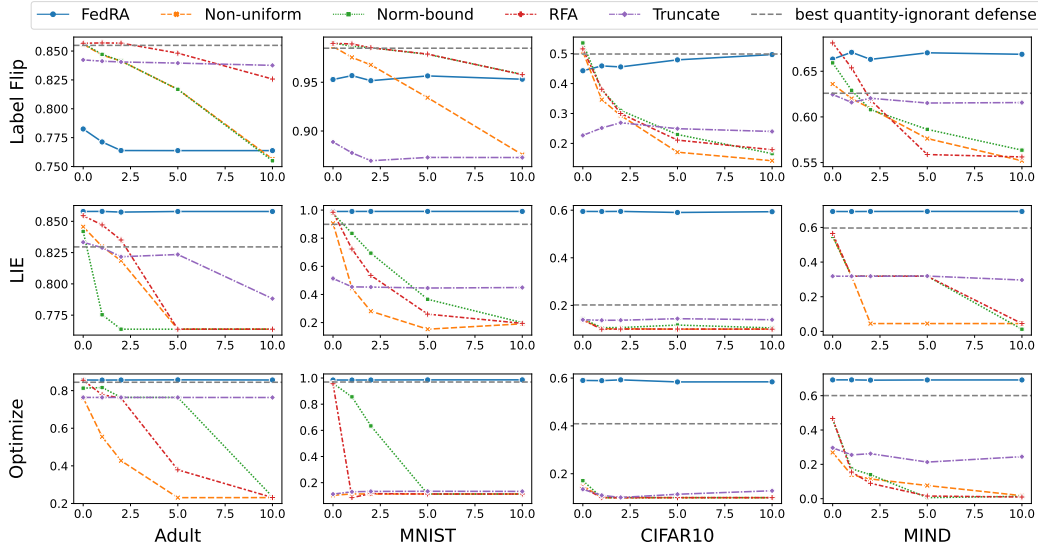


Figure 5: Performance of defenses in the dynamic-ratio non-IID setting. The x-axes are the values of accuracy. The y-axes are the values of quantity-enlarging factors.

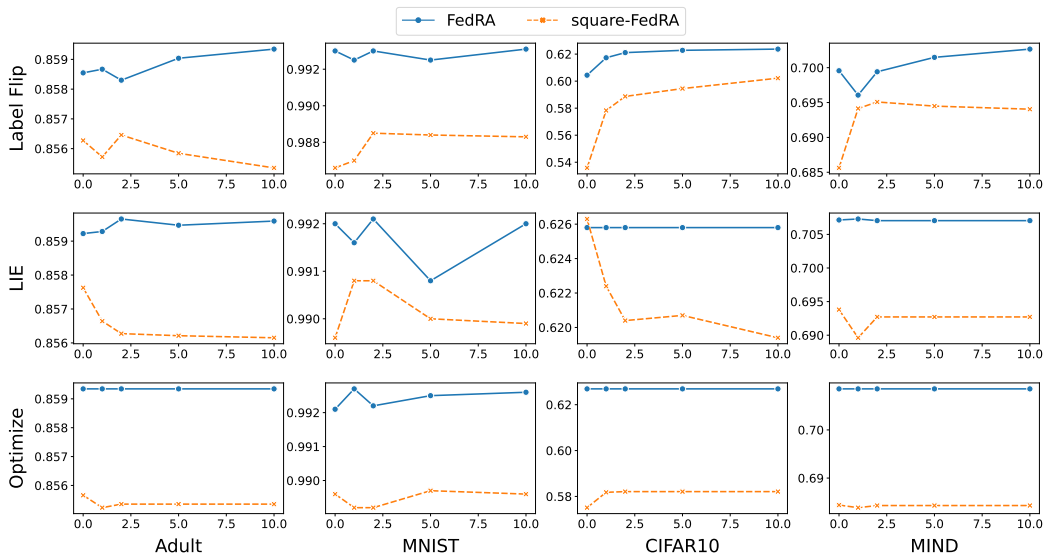


Figure 6: Performance of square-FedRA and FedRA in the fixed-ratio IID setting. The x-axes are the values of accuracy. The y-axes are the values of quantity-enlarging factors.

### C.3 Performance of Square-distance-based FedRA

In this subsection, we compare the performance of square-distance-based FedRA (referred to as square-FedRA) with our  $L_1$ -based FedRA in the fixed-ratio IID setting. The experimental results are shown in Figure 6. Our  $L_1$ -based FedRA outperforms square-FedRA. This may be because, as we proved in Section 4.1 of the main paper, the  $L_1$ -based Krum has a lower upper bound of error  $O(\sqrt{\ln n})$  than the Krum based on square distance  $O(\sqrt{n})$ .

## D Experimental Environments

We conduct experiments on a single V100 GPU with 32GB memory. The version of CUDA is 11.1. We use pytorch 1.9.1.